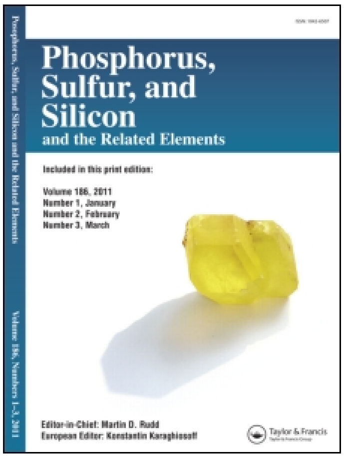

Phosphorus, Sulfur, and Silicon and the Related Elements
Publication details, including instructions for authors and subscription information:
http://www.informaworld.com/smpp/title~content=t713618290

Precursor Routes to Semiconductor Quantum Dots

Mohammad Azad Malik[a]; Paul O'Brien[a]; Neerish Revaprasadu[b]
[a] The Manchester Materials Science Centre and Department of Chemistry, Manchester University, Manchester, UK [b] Department of Chemistry, University of Zululand, South Africa

To cite this Article Malik, Mohammad Azad , O'Brien, Paul and Revaprasadu, Neerish(2005) 'Precursor Routes to Semiconductor Quantum Dots', Phosphorus, Sulfur, and Silicon and the Related Elements, 180: 3, 689 — 712

To link to this Article: DOI: 10.1080/10426500590907426

URL: http://dx.doi.org/10.1080/10426500590907426

Phosphorus, Sulfur, and Silicon, 180:689–712, 2005
Copyright © Taylor & Francis Inc.
ISSN: 1042-6507 print / 1563-5325 online
DOI: 10.1080/10426500590907426

Taylor & Francis
Taylor & Francis Group

Precursor Routes to Semiconductor Quantum Dots

Mohammad Azad Malik
Paul O'Brien
The Manchester Materials Science Centre and Department
of Chemistry, Manchester University, Manchester, UK

Neerish Revaprasadu
Department of Chemistry, University of Zululand, South Africa

Quantum Dots are unique for two very important reasons both of which can potentially be commercially exploited:

- *The electronic and optical properties of Quantum Dots are dependent on the particle size.*
- *As the Quantum Dot nanoparticle becomes smaller the ratio of the number of surface atoms to those in the interior increase. For example in very small particles greater than a third of all atoms reside on the surface. Such a high surface area is useful for catalysis.*

The solutions to the right all contain the same semiconductor material (cadmium selenide, CdSe) but are different colours because unlike the bulk material, which is black, we have controlled the size and therefore the electronic and optical properties (colour) of the Quantum Dots. This property alone can be exploited for the use in a number of technologies such as security tagging and biological probes.

These small particles are one of the inventions spearheading a drive to control of materials with dimensions of the order of nanometres. The potential of the area of nanotechnology as being opened up by interactions between molecular biologists, chemists physisists and almost every type of engineer will be discussed. Applications of such technologies will range from computer chips through display screens to security printing. These new technologies will impact on all of our daily lives. Nanotechnology is attracting attention from all quarters from academia, venture capitalists to the general public. This lecture will explain why the area is both so topical and important.

INTRODUCTION

Research in materials with critical dimensions of the order of nanometers has made a huge impact in the scientific community in the past

Received March 23, 2004; accepted October 5, 2004.

Address, correspondence to Paul O'Brien, The Manchester Materials Science Centre and Department of Chemistry, Manchester University, Oxford Road, Manchester, M139PL, UK. E-mail: paul@obrien@mcn.ac.ulc

decade. The intense interest in these materials is attributed to their unique chemical and electronic properties. These properties make them potentially useful in a wide range of applications, including catalysis, solar cells, biotechnology, and optoelectronics. Synthetic routes to nanoparticles has been of interest to chemists who endeavor to prepare pure, crystalline, surface-derivatised nanoparticles with a narrow size distribution. This review describes and discusses some of these routes to nanoparticles with particular emphasis on the use of organometallic precursors in the preparation of semiconductor nanoparticles.

THEORY

Semiconducting materials with all three dimensions of the range 1–20 nm are referred to in the literature as nanoparticles, nanocrystals, quantum dots (QDs), Q-particles, nanoclusters, or artificial atoms.[1–4] The unique properties of particles in this size range are due to their large surface-to-volume ratio and their reduced dimensions in relation to the excitonic radius of the bulk material. As the particle size is reduced, the ratio of the surface atoms in relation to those in the crystal lattice increases, thereby increasing the significance of the surface in determining the properties of the material. The increase in the band gap of the nanocrystalline material with corresponding reduction of particle size is explained by the phenomenon described as the quantum size effect. This effect is a consequence of the confinement of the charge carriers within the dimensions of the nanocrystals which results in them being treated quantum mechanically as particles in a box. In this novel state of matter the valence band and conduction band split, giving rise to discrete energy levels rather than a continuous band as observed in the bulk material (Figure 1). The close proximity of the electron-and-hole pair in nanosized semiconductors has made it impossible to ignore the Coulombic interaction between the electron and hole and they consequently assume a higher state of kinetic energy than the bulk material. Experimentally, this increase in energy is observed in the optical spectra, where there is blue shift in the band gap as the particle size decreases. The change in color of an optically clear solution of CdSe quantum dots with variation in particle size is shown in Figure 2. In nanocrystalline semiconductors such as CdSe the presence of an excitonic peak or shoulder is also taken as evidence of quantum confinement.[5]

Many model calculations of size quantization effects have been published in the last few years.[6–14] The majority of these calculations start from the macroscopic solid state and determine the increase of the band gap with decreasing particle size on the basis of a particle-in-a-box

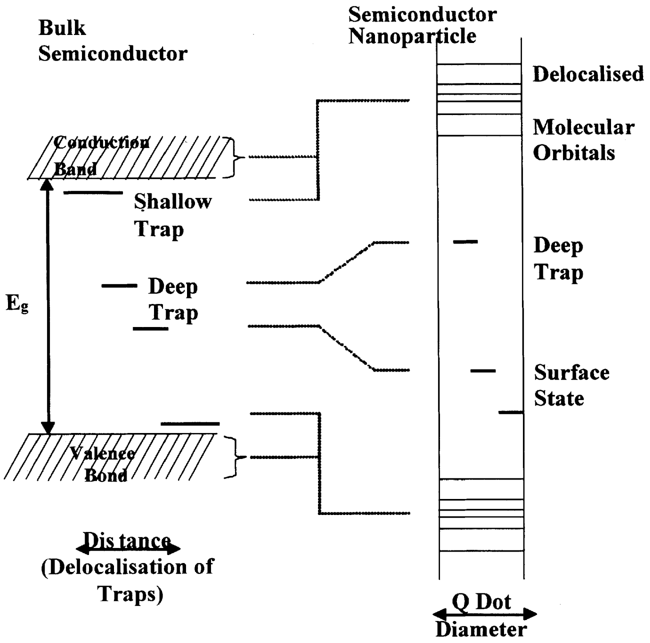

FIGURE 1 Diagram showing the increase in energy and evolution of discrete energy levels in nanocrystalline semiconductors.

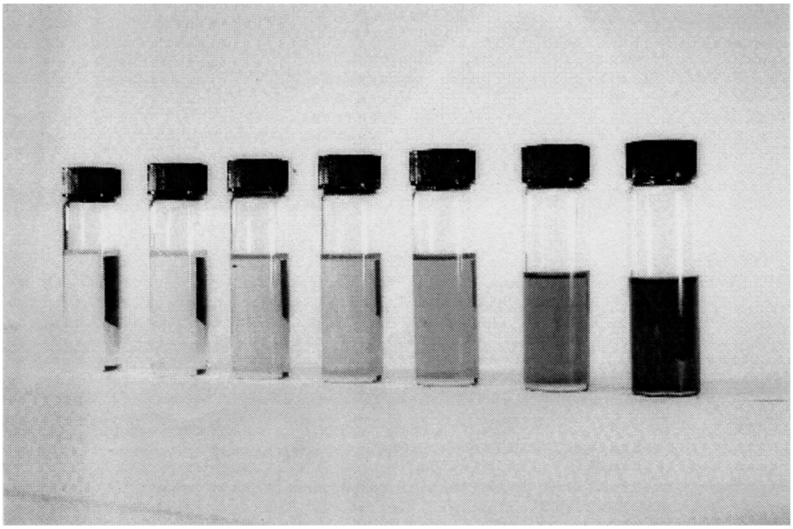

FIGURE 2 Size-selected solutions of CdSe nanoparticles grown from $Cd[Se_2CNMe(CH_2CH2Ph)]_2$.

assumption. The differences in the models lie in the complexity of the calculation and the boundary conditions. Efros et al. described the first calculation.[6] They used spherical, infinite potential wells that ignored the coulombic interactions. Brus et al.[7,8] developed the energy levels of the first excited state by considering the coulombic interactions and polarization terms. On the basis of the effective mass approximation they have developed an equation (1.8) (Eq. (1)) connecting the energy of the first electronic transition of the exciton and the band gap shift with respect to the typical bulk value.

$$\Delta E = \frac{\hbar^2\pi^2}{2R^2}\left[\frac{1}{m_e} + \frac{1}{m_h}\right] - \frac{1.786e^2}{\in R} - 0.248E^*{}_{Ry} \tag{1}$$

Here $m_e{}^*$ and $m_h{}^*$ are the effective mass of the electron and the hole, E^* represents the effective Rydberg energy and the bulk optical dielectric constant, e represents the elementary charge, and R represents the radius of the spherical crystallite. The most universal particle-in-a-box calculation has been presented by Nosaka,[13] whose calculations assume the validity of the effective mass approximation. The appropriate values for the effective masses as well as the high frequency dielectric constants are taken from macro crystalline solids, which result in the uncertainty of these calculations. On the basis of the work by Burdett,[15] Wang[10] described first molecular orbital calculation (tight binding) for Q-particles of PbS, while Lippens et al.[12] did the same for CdS and ZnS. Although they avoid the problem of the effective mass approximation, they do not include the altered bonding forces of the surface atoms as compared to the bulk atoms.

Preparation Methods of Semiconductor Nanoparticles

When atoms or molecules organize into condensed systems, new collective phenomenon develop. The cooperative interactions produce the physical properties we recognize as characteristic of bulk materials. Like atoms or molecules, nanoparticles may also be used as building blocks of condensed matter. Synthetic routes enabling controlled manipulation of nanocrystals into the glassy and ordered states of matter lead to the preparation of close-packed nanocrystalline solids. The assembly of nanoparticles opens up the possibility of fabricating new solid-state materials and devices with novel physical properties, as the interactions between proximal nanocrystals give rise to new collective phenomena.

The chemical methods of producing semiconductor nanoparticles can be divided into four categories, the colloidal route, organometallic route, growth-in-confined matrices, and gas-phase synthesis of nanoparticles.

The colloidal access to quantum dots is achieved by carrying out a precipitation reaction in homogenous solution in the presence of so-called stabilizers.[2] The role of the stabilizers is to prevent agglomeration and further growth of the colloids, thereby keeping them in solution. Brus,[9,16] Weller,[17] and Henglein[18] have used this method to synthesise semiconductor nanoparticles of CdS and ZnS. Their work has contributed significantly towards the understanding of some of the fundamental properties of nanoparticles. Brus reported the synthesis of Q-CdS by mixing aqueous solutions of $CdSO_4$ and $(NH_4)_2S$.[9] By altering the nucleation kinetics using pH, the subsequent size of the nanocrystalline Q-CdS could be controlled. Henglein, Weller, and coworkers studied the photophysical properties of nanocrystalline CdS.[17,18] The analysis of the size distribution revealed that a certain size with the greatest oscillator strength was favored, which corresponds to the optical transition in the absorption spectrum. This was attributed to the existence of magic agglomeration numbers in the size distribution of the sample. Magic agglomeration numbers, integral multiples N of a large number m_0, arise due to the stability of particles with a certain size or because of the kinetics of particle growth. The fast precipitation of the colloids renders a primary size distribution of small particles, peaking at an initial size m_0 (Eq. 2).

$$m_0\mathrm{Cd}^{2+}m_0S^{2-} \rightarrow (\mathrm{CdS})m_0 \tag{2}$$

Growth via Ostwald ripening occurs with the initial size (m_0) and is preserved in the form of integer multiples such as the following (Eqs. 3, 4):

$$(\mathrm{CdS})m_0 \rightarrow (\mathrm{CdS})m_{0-l} + \mathrm{Cd}^{2+} + \mathrm{S}^{2-} \tag{3}$$

$$(\mathrm{CdS})m_0 + \mathrm{Cd}^{2+} + \mathrm{S}^{2-} \rightarrow (\mathrm{CdS})m_{0-l} \tag{4}$$

Nanocrystalline Zn_3P_2 and Cd_3P_2 have been synthesized by the aqueous method by injection of phosphine (PH_3) into a solution containing a metal salt.[18,19]

Q-Cd_3P_2 shows dramatic changes in appearance and electronic properties as the size of the particles is varied. Bulk Cd_3P_2 is black in color whereas nanocrystalline Cd_3P_2 displays a wide range of colors. The smallest colorless particles have a band gap of 4.0 eV (310 nm) with an excitonic peak at 3.93 eV (315 nm). The colloidal route is an efficient one for the preparation of nanosized semiconductor particles. However, certain types of semiconductors such as CdSe, GaAs, InP, and InAs cannot be synthesized easily via this route. The instability of the colloids at high temperatures makes annealing of the particles difficult, thereby making the material poorly crystalline.

The use of confined matrices such as zeolites,[20] layered solids,[21] molecular sieves,[22] micelles/microemulsions,[23,24] gels,[25] and polymers[26–28] is another popular route to nanodimensional particles. Degradation of the host structure upon nanoparticle formation and particle size restrictions due to the host structure are some of the problems associated with this method of synthesis.

Gas phase synthesis of semiconductor nanoparticles involve atmospheric or low pressure evaporation of either powders or the preformed semiconductor, or the coevaporation of the two elemental components, for example, from zinc metal and sulfur.[29] However, the use of these techniques usually resulted in deposits of particles with larger size distributions, in some cases ranging from 10–200 nm. Sercel et al. have reported the synthesis of GaAs nanoparticles by using the organometallic precursor trimethylgallium, $GaMe_3$, which on mixing in a furnace flow reactor with arsine gas, AsH_3, gives crystalline GaAs particles.[30,31] These approaches suffer from the problem of particle aggregation due to the absence of a surface passivating (capping) agent. The only report of gas-phase semiconductor nanoparticle synthesis using a capping agent was by Salata et al. who produced PbS and CdS nanoparticles covered with a polymer layer by reacting a polyvinyl alcohol precursor containing $Pb(NO_3)_2$ or $Cd(NO_3)_2$ in the gas phase with H_2S gas.[32]

PRECURSOR ROUTES

The problems associated with the colloidal route to nanoparticles can be overcome by a method that makes use of organometallic and/or metal organic compounds under anaerobic conditions. Bawendi et al.[5] pioneered this method, whereby good quality, monodispersed, highly crystalline nanoparticles of CdSe, CdS, and CdTe were synthesized. In this method solutions of dimethylcadmium and a chalcogen source were mixed in tri-*n*-octylphosphine (TOP) and injected into hot tri-*n*-octylphosphine oxide (TOPO), a high boiling-point coordinating solvent, at temperatures ranging from 120°C–250°C. The coordinating solvent, TOPO, stabilizes the nanocrystalline colloidal dispersions and electronically passivates the semiconductor surface. The organic surface cap can be replaced by other groups such as pyridine, 4-picoline, tris(2-ethylhexyl)phosphate and 4-(trifluoromethyl)thiophenol. However, subsequent studies have shown that the use of the TOP/TOPO combination to be the most efficient passivating system.

The TOPO method has advantages over other synthetic methods, including near monodispersity, increased crystallinity, and high yields. The surface nature of CdSe/TOPO nanocrystallites has been studied by nuclear magnetic resonance spectroscopy and X-ray photoelectron spectroscopy.[33] For these methods the surface coverage, the percentage of surface sites bound to TOPO molecules through a metal–oxygen dative bond, increases from 30% (d ≈ 60 Å) to 60% (d ≈ 18 Å) as the particle size decreases. Steric effects can explain variations in surface coverage with particle size. The interaction between surface bound bulky neighbouring capping molecules (TOPO) predominates in larger particles while smaller particles can accommodate higher percentage levels of surface coverage due to less steric hindrance.[33]

However, the use of dimethylcadmium, a volatile and highly toxic substance, is a limitation to this method. There have been reports on the investigation of replacing dimethylcadmium as a common precursor for the synthesis of CdSe nanoparticles. Stable, less volatile organometallic cadmium compounds can replace dimethylcadmium. Di-neopentylcadmium, bis(3-diethylaminopropyl)-cadmium and (2,2′-bipyridine)dimethylcadmium have been successfully used as a cadmium source for the preparation of TOPO capped CdSe nanoparticles.[34] A modification of the conventional TOPO method was reported by Alivisatos et al.,[35] whereby II–VI semiconductor nanoparticles were synthesized by a method that avoids the use of metal alkyls. In a typical preparation, TOPO capped InP nanoparticles were synthesized by reacting $InCl_3$ with $P(SiMe_3)$ in hot TOPO, with subsequent annealing of the particles in dodecylamine. The InP nanoparticles were of 20 Å–50 Å with TOPO coverage ranging from 30–100 %. For InAs, prepared by a similar TOPO method, using the dehalosilylation reaction between $As(Si(CH_3)_3)_3$ and $InCl_3$, surface oxidation did not change the properties of the resultant particles.[36]

III/V semiconductors do not crystallize as easily as II/VI materials because of their increased covalent nature. Solid-state metathesis reactions have been used as a route to III–V compounds.[37] InAs and InP were synthesized by heating the products of the independent 1:1 mole ratios of InX_3 (X = Cl, Br, I) with $As(SiMe_3)_3$ and $P(SiMe_3)_3$ respectively, and the 2:1 mole ratio of $InCl_3$ with $As(SiMe_3)_3$.[38] The dehalosilylation reaction of $InCl_3$ and $As(Si(CH_3)_3)_3$ at a temperature of 265°C produced InAs nanoparticles, with TOP and TOPO serving as solvents.[39,40] Alivisatos et al.[41] reported the preparation of GaAs nanoparticles using $GaCl_3$ and $As(SiMe_3)_3$ in quinoline. The dehalosilylation reaction also has been used as a route to prepare III-antimonide nanoparticles.[42] GaSb nanoparticles in the 20–30 nm size range were reported to be synthesized by the reaction between $GaCl_3$ and $Sb(SiMe_3)_3$.

SINGLE MOLECULE PRECURSORS

Single molecular precursors containing the metal and nonmetal chalcogenides were initially used by O'Brien et al. to produce thin films by metal organic chemical vapor deposition (MOCVD).[43–45] These

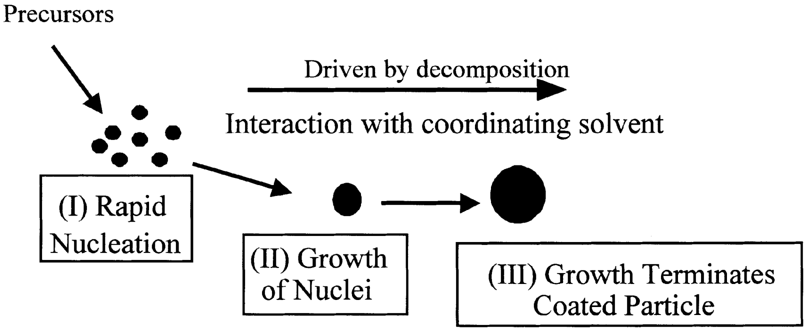

FIGURE 3 Scheme showing the various stages of nanoparticle growth using the one-pot synthetic method.

compounds containing the metal and chalcogenide were considered to be versatile as a source for nanoparticle growth. Trindade and O'Brien first reported the use of cadmium dithio- and diseleno-carbamate complexes as precursors for the preparation of TOPO capped II–VI materials.[46,47] The method of nanoparticle synthesis involves the dispersion of the single source precursor in TOP, followed by injection into hot TOPO (250°C). The general scheme of nanoparticle synthesis using single molecule precursors is shown in Figure 3. The formation of the nanoparticles is consistent with the LaMer mechanism for colloids.[48] The decomposition of the precursor drives the formation of the nanoparticles with termination of growth occurring when the precursor supply is depleted. After the initial injection there is a rapid burst of nucleation, which is followed by controlled growth of the nuclei by Ostwald ripening. The resultant nanoparticles are passivated by TOPO, which prevents agglomeration. The nanoparticles are isolated by a process whereby a nonsolvent (methanol) is added to the reaction mixture, which increases the average polarity of the solution and consequently decreases the energy barriers to flocculation. The flocculant precipitate obtained is separated by centrifugation and redispersed in toluene to give an optically clear solution of TOPO-capped nanoparticles.

II–VI QUANTUM DOTS

Various II–VI semiconductor quantum dots have been synthesized using single molecule precursors. Initially the thermolysis of $Cd(S_2CNEt)_2$ in TOPO resulted in high quality nanoparticles of CdS.[46,47] However, the selenium analogue produced microsized particles of selenium.[49] The subsequent use of compounds of the formula $RCd(E_2CNEt_2)$ (Figure 4), (R = neopentyl, Me; E = S,Se) led to the synthesis of good quality, close to monodispersed CdS and CdS nanoparticles.[46,47] $Pb(Se_2CNEt_2)$

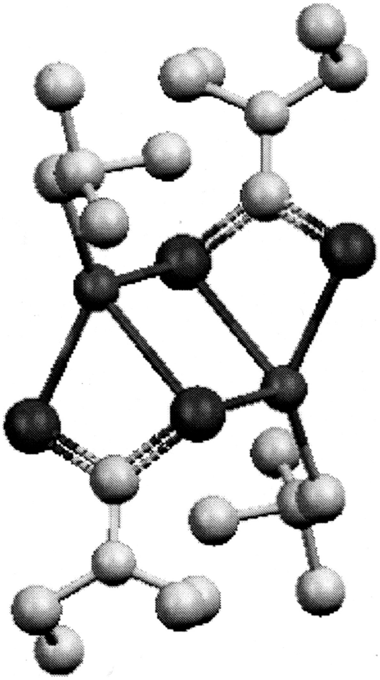

FIGURE 4 X-ray structure of [$NpCd(Se_2CNEt_2)$].

and $Cu(Se_2CNEt_2)$ were used to prepare PbSe[50] and CuSe[51] nanoparticles respectively. Revaprasadu et al.[39,40] reported the use of the single molecule complex of $[EtZn(E_2CNEt_2)]_2$(E = S,Se) (Figure 5) in TOPO to prepare crystalline nanoparticles of ZnE. An attempt by Hines and Guyot-Sionnest to use TOPO/TOP as the passivating agents failed. Instead the TOPO/TOP was replaced by a mixture of hexadecylamine and TOPO.[52]

The use of dithio-/diseleno-carbamato complexes of cadmium/zinc containing asymmetrical alkyl groups has proven to be the precursors that give nanoparticles of the highest quality. These precursors are non-air sensitive, stable for a period of months, easy to synthesize, and most of all pyrolyse cleanly to give the highest yield. Previous investigations showed that subtle changes in substituents at the nitrogen of a diseleno- or dithio-carbamate can markedly affect the thermal decomposition of metal complexes used in the preparation of chalcogenides.[53] The formation of stable ring structures might be expected to be enhanced by having greater stabilizing substituents at the β-carbon to the nitrogen (eg. bulkier alkyl groups), so when the ring forms it may cleanly eliminate. Studies by GC-MS and EI-MS show the

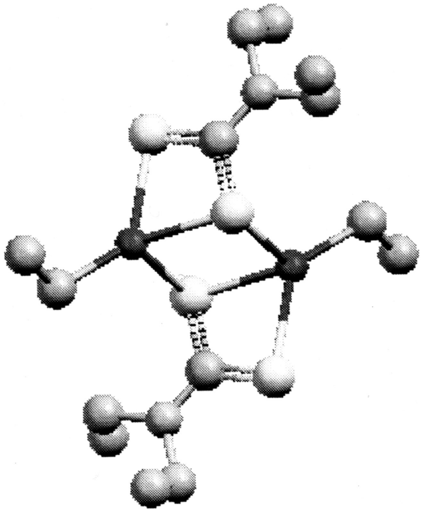

FIGURE 5 Structure of ethyl(dithyldiselenocarbamato)zinc(II).

reason why elemental selenium is deposited with the metal selenide from the compounds such as $M(Se_2CNEt_2)_2$ [M = Zn or Cd] whereas $M(Se_2CNMeHex)_2$ [M = Zn, Cd] and $EtZnSe_2CNEt_2$ give clean deposits of metal selenides (Figure 6). The formation of selenium clusters Se_n n = 1–7 is observed on the pyrolysis of diethyl-derivatives whereas no selenium clusters were observed for methyl-hexyl or mixed alkyl derivatives.

TOPO-capped CdS and CdSe nanoparticles were synthesized at 250°C using $[Cd(S_2CNMeHex)_2]$ and $[Cd(Se_2CNMeHex)_2]$ as the precursors[54,55] The as prepared nanoparticles showed blue shifts in their optical spectra in relation to the bulk material. The optical spectra of CdSe showed well-defined excitonic features and the corresponding photoluminescence spectrum was Stoke's shifted in relation to the band edge. The X-ray diffraction of CdS showed broad diffraction peaks, typical of nanometric materials with a predominance of the hexagonal phase. The TEM images showed well-defined, close-to-spherical particles and the lattice fringes of the high resolution. TEM images confirmed their crystalline nature (Figure 7). In their time-growth study on CdSe nanoparticles, O'Brien et al.[55] showed that particle growth is linear with time (10 min. to 24 h). However, there is a decrease in the standard deviation from $\pm 12.93\%$–$\pm 8.69\%$ from the ($t = 10$ min) to the ($t = 30$ min) sample, which indicates a narrow size distribution. The particle size distribution then increases over 24 hrs ($\sigma = \pm 10.13$). This trend has been reported previously for CdSe

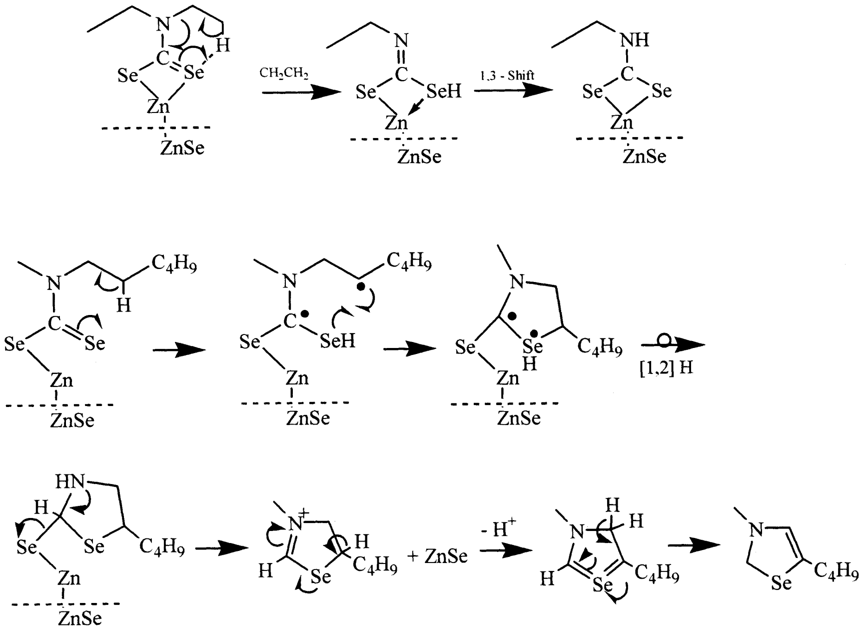

FIGURE 6 Decomposition mechanism of bis(Hexy(methyl)diselenocarbamato)zinc(II).

nanoparticles by Alivisatos et al.[56] who explained the phenomenon on the basis of classical colloidal chemistry. The initial decrease in size distribution occurs when the CdSe nanoparticles are larger than the critical size at equilibrium, which results in faster growth of smaller

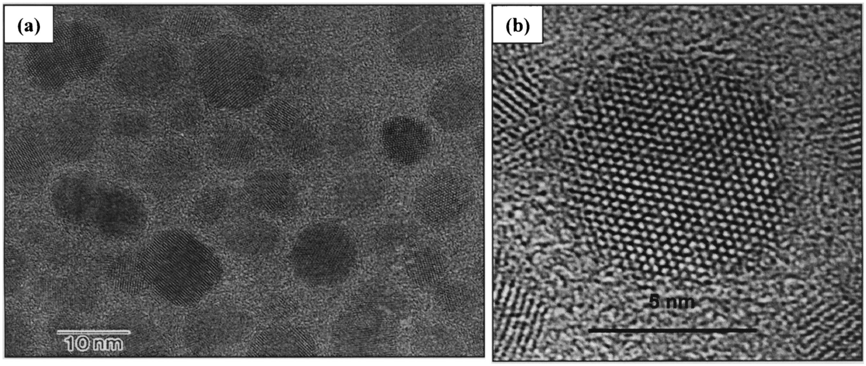

FIGURE 7 CdSe nanoparticles. (a) HRTEM image showing an array of nanoparticles and (b) single quantum dot (ca. diameter = 5 nm).

particles in relation to larger particles. The size distribution broadens again when the precursor supply is depleted. This happens because the critical size becomes larger than the average size, which results in the collapse of smaller nanoparticles while larger particles continue to grow.

Recently [$Pt(S_2CNMe(Hex))_2$] and [$Pd(S_2CNMe(Hex))_2$] have been used for the synthesis of TOPO capped PtS (*ca.* 3 nm diameter) and PdS (*ca.* 5 nm diameter) nanoparticles.[57] These precursors were also used to deposit thin films of PdS and PtS on GaAs substrates by low-pressure metal-organic chemical-vapor deposition (LP-MOCVD). The PtS nanoparticles exhibit a strong excitonic peak at 360 nm in the absorption spectra with the band edge at 410 nm, whereas the band edge of the PtS nanoparticles was found to be at 455 nm. The emission maxima of PtS (495 nm) and PdS (465 nm) are red-shifted in relation to their band edges. The thin films of the PtS and PdS were characterized by X-ray Diffraction (XRD), Energy Dispersive Analytical XRD (EDAX), and Scanning Electron Microscopy (SEM) methods. The platinum and palladium complexes appeared to be less volatile when compared to the corresponding zinc and cadmium complexes and hence required higher deposition temperatures with slower growth.

Most of the single source precursors for II/VI nanoparticles were based on dithio-/diseleno-carbamato system but recently other complexes have been synthesized and used for the preparation of nanoparticles. Cadmium(II) complex of N,N′-bis(thiocarbamoyl)-hydrazine, $Cd(SCNHNH_2)_2Cl_2$, was used as a precursor for the synthesis of CdS nanoparticles.[58,59] The $Cd(SCNHNH_2)_2Cl_2$ was thermolyzed in hot TOPO (230°C) to give TOPO-capped CdS nanoparticles with an average diameter of 5.05 nm ±8%. The particles displayed a band edge at 478 nm (2.59 eV), a blue shift of 37 nm in relation to bulk material (515 nm). The photoluminescence spectrum of the CdS showed close to band edge emission, with the maximum at 450 nm ($\lambda_{exc.} = 380$ nm). The other system which has the potential of single source precursors is xanthate.[59] The closeness in structure of xanthates compared to dithiocarbamates implies that xanthates are expected to resemble dithiocarbamates in its bonding mode. Cadmium ethylxanthate was thermolysed in TOPO at 160° to give monodispersed TOPO capped CdS nanoparticles.[59] The XRD pattern shows the material to behexagonal with a calculated particle size (from Scherrer equation) of 3.9 nm. The TEM image shows well defined, spherical particles with an average size of 4.2 nm ± 10%. The particle growth was also monitored by absorption spectroscopy. The absence of significant changes in the optical absorption spectra of samples isolated after 5, 10, 30 and 1 h is an indication that

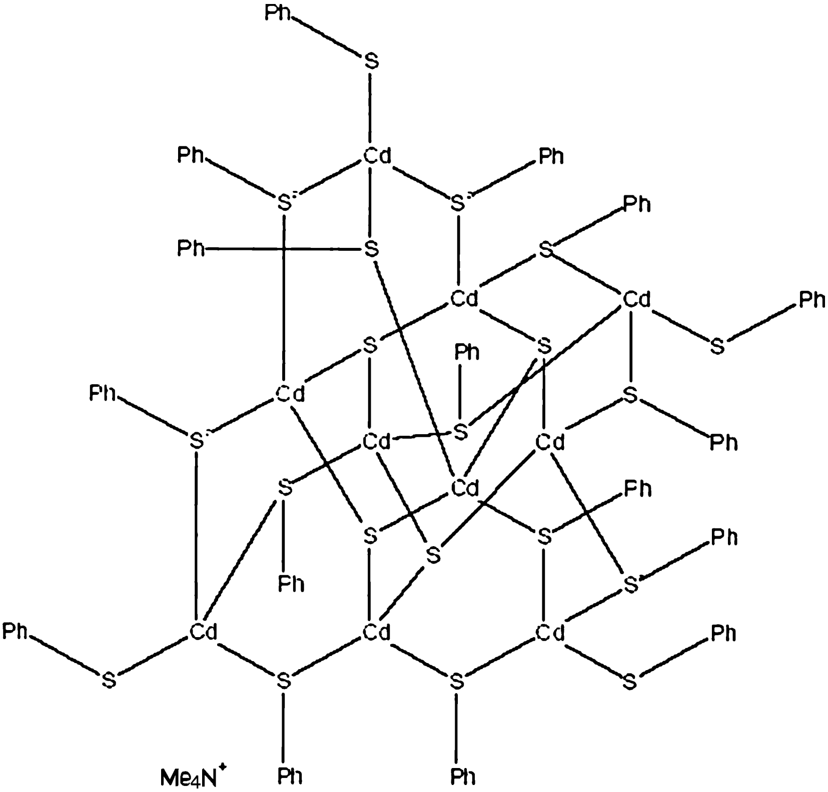

FIGURE 8 $Me4N[Cd_{10}S_4(SPh)_{16}]$.

nucleation and growth takes place very rapidly at the temperature of injection.

Air-stable inorganic–molecular clusters (e.g. $[M_{10}Se_4(SPh)_{16}]^{4+}$ where M = Cd or Zn) (Figure 8) have been reported as single-source precursors towards highly monodispersed nanoparticles.[60] It has been demonstrated that selenocarbamates such as $M_n(Se_2CNR^1R^2)_n$[61,62] are excellent for the synthesis of group 12 chalcogenides but the diselenocarbamato ligand is prepared from toxic and noxious carbon diselenide. Imino-diisopropylphosphineselenides are prepared by the oxidative insertion of elemental selenium.[60] The cadmium imino-bis(diisopropylphosphine selenide) compound, $Cd[N(SeP^iPr_2)_2]_2$ (Figure 9), was first synthesised by Woollins et al.[62] from diisopropylchlorophosphine via a two-step strategy. Improved yields for $Cd[N(SeP^iPr_2)_2]_2$ above those reported[63] can be afforded by utilizing $CdCl_2$/NaOMe conditions rather than metal carbonates. Sodium

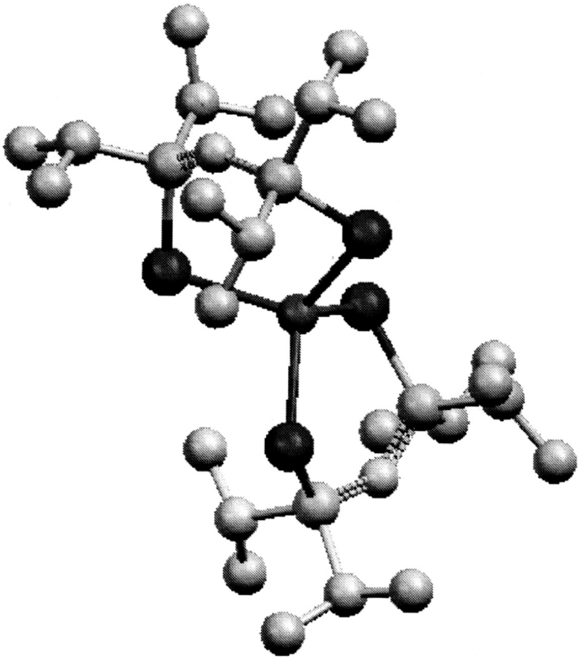

FIGURE 9 Molecular structure of $Cd[N(SeP^{i}Pr_2)_2]_2$.

methoxide (0.56 g, 9.82 mmol) was added to a stirred solution of $NH(SeP^{i}Pr_2)_2$ (4g, 9.82 mmol) in anhydrous methanol (100 cm^3). The resulting pink solution was stirred at room temperature for 10 min. Cadmium chloride (0.90 g, 4.91 mmol) was added yielding an immediate off-white precipitate. The suspension was stirred at room temperature for 2 h. The recovered solid was washed with methanol (100 cm^3) and dried under vacuum. Recrystallization from chloroform/methanol yielded 4.51 g (99%) of white crystals. Imino-bis(dialkylphosphineselenide) complexes have recently been used as CVD precursors.[64,65] The $NH(SeP^{i}Pr_2)_2$ ligand is more thermally stable than bulky selenolate ligands, such as $[SeSi(SiMe_3)_3]^-$, and thermolysis of its complexes produces cleaner products with reduced contamination caused by undesired ligand degradation reactions.[66,67] One-step size-controlled synthesis of QDs was carried by the thermolysis of $Cd[N(SeP^{i}Pr_2)_2]_2$.[68,69] In the synthesis of CdSe, the sizes of QDs derived from $Cd[N(SeP^{i}Pr_2)_2]_2$ can accurately be varied by the length of the reaction time. The dots luminesce in the visible region of the electromagnetic spectrum and the emission wavelength vary over a wide range (up to 650 nm) depending on the particle size.

PARTICLE MORPHOLOGY

It is a challenge to many chemists to synthesize nanoparticles with varying shapes and sizes. Recently there has been interest in the synthesis of rod-shaped nanoparticles with controllable shape and size in the quantum confinement range.[70–76] Semiconductor nanoparticles with rod-like structures were prepared by Alivisatos et al.[76] who added Hexylphosphonic Acid (HPA), an impurity actually present in commercial TOPO. Peng studied various factors that influence the formation of nonspherical morphology for CdSe nanoparticles.[71] Their studies have shown that the nature of precursor, rate of nucleation, and nature of the coordinating solvent/surfactant are the critical factors that affect the particle morphology. The CdE nanoparticles were synthesized using CdO and $Cd(OAc)_2$ ($OAc = O_2CCH_3$) together as an alkylphosphonic acid. The study shows the rod shaped particles when the monomer concentration is high in the reaction environment. At intermediate monomer concentrations the nanoparticles grow simultaneously in three dimensions and a mixture of spherical and rods are obtained. At low monomer concentrations the particles are exclusively spherical.

$$\mathrm{CdR} + \mathrm{TDPA} + \mathrm{TOPO} \xrightarrow[\mathrm{E/TOP/Toluene}]{\Delta} \mathrm{CdE^{o}}$$

$$\mathrm{R} = \mathrm{O}, (\mathrm{OAc})_2 \qquad \mathrm{E^{o}} = \mathrm{S, Se, Te}$$

$$\mathrm{E} = \mathrm{S(SiMe_3)_2, Se, Te}$$

$$\mathrm{TDPA} = \text{teradecylphosphonic acid}$$

SCHEME 1 Synthesis of Cadmium chalcogenides.[74]

Colvin et al.[74] also used CdO and $Cd(O_2CCH_3)$ to synthesize CdS, CdSe, and CdTe nanoparticles (Scheme 1). The CdS particles are spherical in shape, while the CdSe and CdTe are reported to have rod-like and tetrapod-like morphologies. CdS nanorods also have been synthesised by thermolyzing cadmium ethylxanthate in hot Hexadecylamine (HDA) solution.[59] The effects of reaction conditions such as reaction temperature, precursor concentration, and reaction time on the particle morphology were investigated. The findings confirmed the earlier work by Peng,[57] i.e., low monomer concentration produces spherical shaped particles while a high monomer concentration favors the rod-shaped particles. The synthesis of CdS nanorods by the thermolysis of a thiosemicarbazide complex of cadmium, $[Cd(NH_2CSNHNH_2)_2Cl_2]$ in TOPO has been reported.[70] Nanodimensional particles of CdS with lengths in the range of 10–24 nm and diameters in the range 3–5 nm are visible in

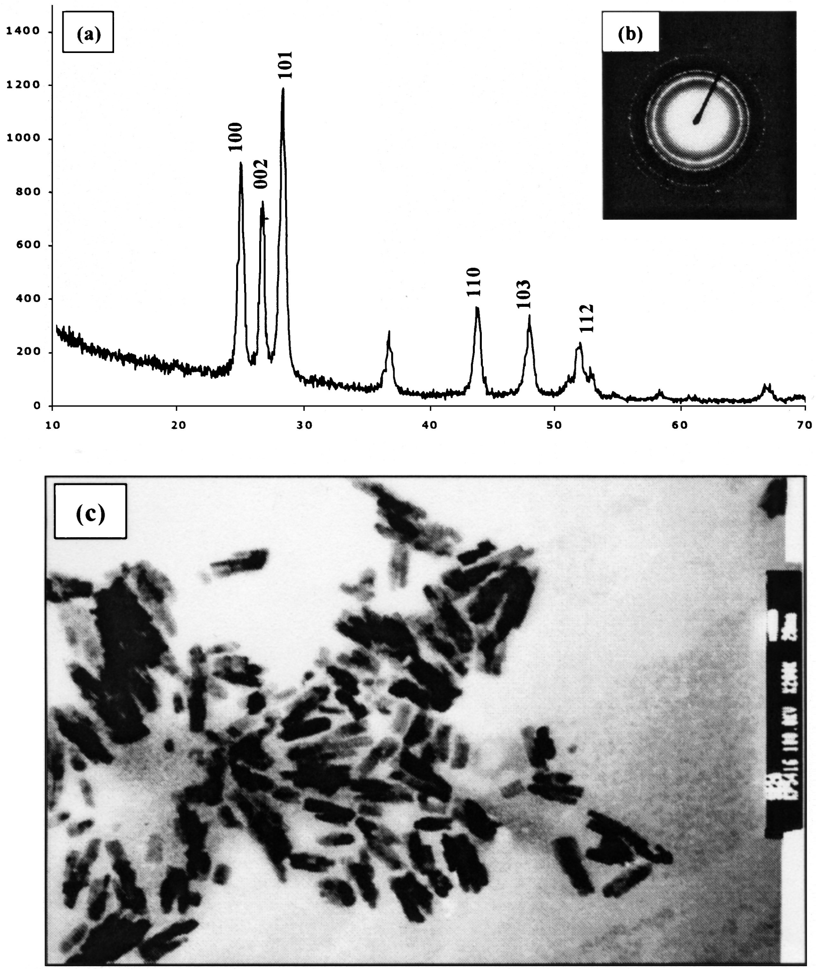

FIGURE 10 CdS nanorods. (a) X-ray diffraction pattern, (b) selected area diffraction pattern, and (c) transmission electron microscope image showing the rod-like particle shape.

the TEM images (Figure 10). We also are investigating the effect of the precursor and passivating group on the morphology of the particles. Recently PbSe were reported to be prepared by reacting lead cyclohexanebutirate and tributylphosphine/selenium precursors in TOPO/tributyl-phosphine at 118°C.[75] At low precursor concentration separated nanoparticles of PbSe were formed. An increase in concentration and temperature enabled the formation of polycrystalline spherical assemblies (after 10–60 min.) or wire-like ordered assemblies (after 90 min.)

III-V QUANTUM DOTS

The use of single-source precursors containing the metal–pnictide bond is an attractive route to III-V nanoparticles. Wells et al.[78] reported the synthesis of GaAs and GaP using single molecule precursors. GaAs was obtained from $AsCl_3Ga_2$, prepared from the reaction of $GaCl_3$ and $As(SiMe_3)_3$ at room temperature.[64] The decomposition of $[Cl_2GaP(SiMe_3)_2]_2$ at 300°C synthesized from the reaction of $P(SiMe_3)_3$ and $GaCl_3$ produced impure GaP. Following the successful synthesis of InAs nanoparticles from $InCl_3$ and $As(NMe_2)_3$ by Green et al.,[79] a similar route was adapted to prepare GaAs nanoparticles.[80] Recently and for the first time, GaAs[81] and InAs[82] nanoparticles were synthesized from a single source precursor $[^tBu_2AsMMe_2]_2$ (M = Ga or In) (Figure 11).

A single-molecular approach was also employed to produce III–V nanoparticles of InP and GaP, using the indium/gallium

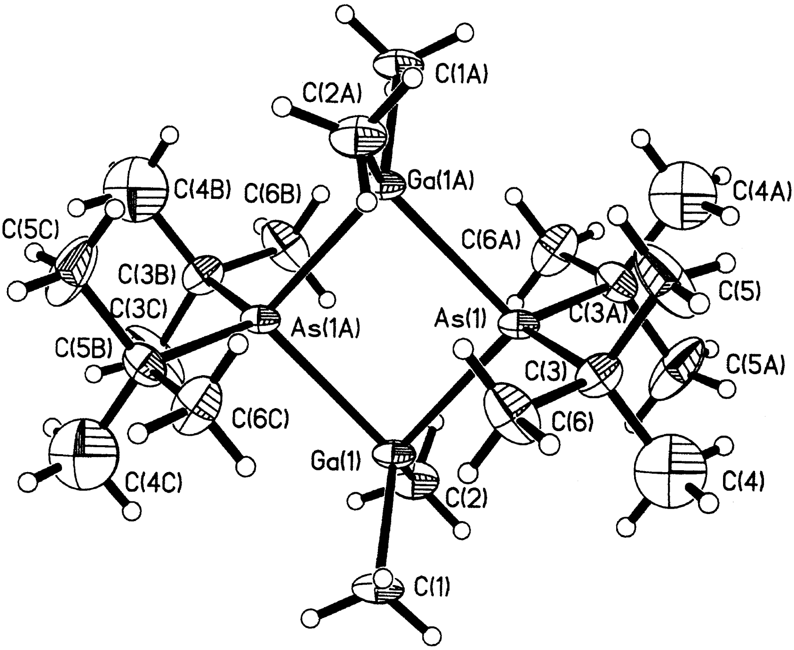

FIGURE 11 Molecular structure of $[^tBu_2AsGaMe_2]_2$.

diorganophosphide compounds, $M(P^tBu_2)_3$ (M = Ga,In), which were dissolved in 4-ethylpyridine (solvent and capping agent) and refluxed for 7 days.[83] For InP, the resulting nanoparticles show blue shifts in their electronic spectra (band edge = 1.92 eV) as compared to the corresponding band gap (1.27 eV) of the bulk material. The product consisted of relatively monodispersed nanoparticles with an average size of 7.24 nm. Green et al.[84,85] have also reported the use of the diorganophosphide compounds, $[MeCdP(Bu^t_2)_3]$ and $[MeCd(\mu\text{-}PPh_2)]_3(HPPh_2)$, as a precursors for the synthesis of Cd_3P_2 nanoparticles. The TOPO-capped and 4-ethylpyridine-capped Cd_3P_2 nanoparticles show pronounced size quantization effects due to their large-bulk excitonic diameter. The TOPO-capped Cd_3P_2 nanoparticles are more stable against photodegradation unlike those prepared by the colloidal route, which are air-sensitive and decompose upon illumination. Micic found that the reaction of metal salts with oxalate complexes were effective starting materials for crystalline nanoparticles.[86] Wells investigated the use of cyclotrigallazanes, such as $[H_2GaNH_2]_3$, as precursors to GaN nanoparticles.[87] Frank et al. reported the preparation of hexagonal GaN nanoparticles by detonation of gallium azides.[88] Surface passivated GaN nanoparticles also have been reported by Micic, whereby polymeric precursors $[Ga(NH_{3/2})]_n$ were thermolyzed in trioctylamine.[89] Another route to GaN nanoparticles is the metathesis reaction between gallium chloride and sodium azide.[90] It must be noted that extra precautions must be taken when handling the metal azides as they are thermally unstable and potentially explosive. One of the advantages of using single molecule precursors as a route to III–V nanoparticles is the increased stability of precursors in relation to the starting materials making the preparation of the quantum dots easier. Although the synthesis of main group pnictides has been developed, there has been relatively little work on transition metal pnictides. Iron phosphide nanoparticles have been reported to be synthesized by annealing the iron phosphide precursor on atomically flat mica surfaces.[76] At 700°C, iron phosphide particles ranging from 0.8–37 nm were deposited.

Mn DOPED QUANTUM DOTS

There has been a considerable interest in the synthesis of doped semiconductors owing to their novel optical and transport properties, which makes them potentially useful for technological applications. The doping of manganese gives a new class of II–VI semiconductor nanoparticles.[92–104] These reports suggest the drastic changes in optical properties in the doped nanocrystals are clearly related to the nature and local structure of the luminescent center in the material. If one considers a 0.5% level of Mn doping in a nanosized ZnS particle with diameter around 3 nm, on average there is only a single Mn impurity center within such a ZnS host. Because of the small size of the system, this single impurity center could give rise to significant changes in the physical properties as a result of symmetry breaking, size quantization, and hybridization of host *sp*-states with *d* states of Mn. Mn doped ZnS and CdS quantum dots have orange luminescence which is attributed to the spin forbidden $^4T_1$–$^6A_1$ electronic transition of Mn.[92–94] ZnS nanocrystals doped with Mn showed a large increase in external photoluminescent quantum efficiency with decreasing nanocrystal size and a shortening of the lifetime of the transition associated with the impurity. These results were attributed to a strong hybridization of the *sp*-electron states of the host material (ZnS) with the *d*-electron states of the impurity (Mn). The crystal fields experienced by Mn impurities near the surface of the nanocrystal will be significantly different from those in bulk ZnS. These also would enhance the radiative rate for the internal transition. As mentioned above, the location of the Mn is also important in deciding the optical properties. Murphy et al.[93] reported that manganese-doped ZnS gave orange emission (585 nm) whereas the ZnS particles with Mn on the surface emit in the ultraviolet (435). The local structure of these particles has been studied by TEM, XRD, Energy Dispersion Spectroscopy (EDS), Electron Paramagnetic Resonance (EPR) and Near-Edge X-ray-Absorption Fine Structure (NEXAFS).

The colloidal route is the most common route used to synthesize Mn-doped ZnS or CdS nanoparticles. Recently Bawendi and coworkers reported the synthesis of TOPO-capped Mn-doped CdSe using two different manganese precursors.[102] The use of manganese salts produced CdSe particles with the manganese on the surface whereas the use of an organometallic complex, $[Mn_2(\mu\text{-}SeMe)_2(CO)_8]$, resulted in manganese being incorporated in the lattice. Our group has reported the synthesis of Mn-doped ZnS and CdS nanoparticles using $[Zn(S2CNEt_2)_2]$ and $[Cd(S_2CNMeHex)_2]$ $MnCl_2$.[103,104] The Electron Spin Resonance (ESR) spectra for both the Mn-doped ZnS and CdS nanoparticles show some weak partially resolved peaks superimposed on a broad background signal. These spectra are characteristic of manganese (II) ions in tetrahedral sites which could be attributed to manganese incorporated into the crystal lattice. A decrease in the resolution of the fine structure was further observed for the EPR measurements of Mn-doped CdS nanoparticles carried out a week later. This change is not observed for Mn-doped ZnS. This effect has been explained by taking into account the ionic radius of manganese, zinc, and cadmium. The difference in ionic radii between manganese (ionic radius = 80 pm) and cadmium (ionic radius = 92 pm) causes a disturbance in the crystal lattice whereas the comparable radii of manganese and zinc (ionic radius = 74 pm) causes less perturbation.

CORE-SHELL TYPE NANOPARTICLES

The modification of the surface of nanoparticles has been intensively investigated. Passivation of the surface has been achieved by the capping of the nanoparticles by organic and inorganic materials. The epitaxial growth of a shell of a second material on a core of another material to form a core-shell particle is also a successful approach in achieving efficient passivation.[105–112] When compared to the uncoated parent material, the core-shell nanoparticles exhibit increased luminescence quantum yields and decreased fluorescence lifetimes. O'Brien et al.[111,112] reported a simple route to CdSe/CdS, CdSe/ZnS, and CdSe/ZnSe core/shell and CdSe/CdS composites using bis(hexyl(methyl)dithio-/-diselenocarbamato)-cadmium(II)/zinc(II) compounds as single source precursors. In a typical preparation, CdSe/CdS core-shell nanoparticles, a solution of [Cd(S_2CNMeHex)$_2$] in TOP was injected into a deep red mixture of [Cd(Se_2CNMeHex)$_2$] in TOP/TOPO, which had previously been injected into hot (250°C, 30 min.) TOPO solution. The red shift in the absorption spectra of the core-shell material in relation to the CdSe and the increased intensity of the photoluminescence spectra are evidence of shell growth. Furthermore, the XRD patterns show sharp peaks which suggest that the shell is crystalline and epitaxially grown on the CdSe core. The CdSe-CdS composites were prepared by dissolving [Cd(Se_2CNMeHex)$_2$] and [Cd(S_2CNMeHex)$_2$] in TOP and the resultant mixture injected into TOPO (250°C, 30 min.). The shift in the peaks in the XRD pattern to lower 2θ values and the blue shift in the optical spectra are evidence for composite formation.

CONCLUSIONS

Although a wide range of synthetic methods have been reported for the preparation of quantum dots of semiconductor materials, it seems clear that there is still a problem associated with the reproducible preparation of robust materials required for technological applications.

Colloidal routes have problems with reproducibility and instability. Colloidal methods use low temperature and in general the crystallinity of the material is poor. However, for certain materials, especially soft ones, this approach may be advantageous. Reactions in confined spaces, for example, within zeolites, micelles, or biological materials, might be an interesting extension of this method.

The use of higher temperature methods, typically using processing temperatures in the range of 200–300°C, has intrinsic advantages. Good quality samples of various nanoparticles are readily prepared using routes based on thermolytic reactions in TOPO or related solvents. Several groups have been involved in developing such chemistry. For semiconductor materials, the majority of simple prototype devices have been made from materials prepared by these methods. The use of single-source precursors is an extension of these methods, which has proven to be a useful method in many cases. Single-source precursors have the advantages of being less toxic, insensitive to air and moisture, and easier to purify (which may prove to be a major issue as impurities may drastically change the intended electronic properties), with preparations generally undertaken at lower temperatures. There is no generally used method for the manufacture of defined robust nanoparticle materials. The unique properties of these materials, especially the possibilities for band gap, tailoring, and tuned luminescence, may lead to their potential use in many future technologies.

REFERENCES

[1] T. Trindade, P. O'Brien, and N. Pickett, *Chem. Mater.*, **13,** 3843 (2001).
[2] A. Eychmuller, *J. Phys. Chem. B*, **104,** 6514 (2000).
[3] C. B. Murray, C. R. Kagan, and M.G. Bawendi, *Annu. Rev. Mat. Sci.*, **30,** 545 (2000).
[4] A. Henglein, *A. Chem. Rev.*, **89,** 1861 (1989).
[5] C. B Murray, D. J. Norris, and M. G. Bawendi, *J. Am. Chem. Soc.*, **115,** 8706.
[6] A. L. Efros and A. L. Efros, *Sov. Phys. Semicond.*, **16,** 772 (1982).
[7] L. E. Brus, *J. Chem. Phys.*, **79,** 5566 (1983).
[8] L. E. Brus, *J. Chem. Phys.*, **80,** 4403 (1984).
[9] R. Rossetti, J. L. Ellison, J. M. Gibson, and L. E. Brus, *J. Chem. Phys.*, **80,** 4464 (1984).
[10] Y. Wang and N. Herron, *Phys. Rev. B. Condens. Matter*, **42,** 7253 (1990).
[11] Y. Kayanuma, *Phys. Rev. B.: Condens. Matter*, **38,** 9797 (1988).
[12] P. E. Lippens and M. Lanoo, *Phys. Rev. B. Condens. Matter*, **39,** 10935 (1989).
[13] Y. Nosaka, *J. Phys. Chem.*, **95**, 5054 (1991).
[14] M. V. Rama Krishna and R. A. Friesner, *J. Chem. Phys.*, **95,** 8309 (1991).
[15] J. K. Burdett, *Prog. Solid State Chem.*, **15,** 173 (1984).
[16] R. Rossetti, R. Hull, and J. M. Gibson, *J. Chem. Phys.*, **82,** 552 (1985).
[17] H. Weller, *Adv. Mater.*, **5,** 88 (1993).
[18] H. Weller, A. Fojtik, and A. Henglein, *Chem. Phys. Rev.*, **117,** 485 (1985).
[19] H. Haase, H. Weller, and H. Henglein, *Ber. Bunsen-Ges. Phys. Chem.*, **92,** 1103 (1988).
[20] Y. Wang and N. Herron, *J. Phys. Chem.*, **91,** 257 (1987).
[21] T. Cassagneau, G. B. Hix, D. J. Jones, P. Maireles-Torres, M. Romari, and J. Roziere, *J. Mater. Chem.*, **4,** 189 (1994).
[22] G. Glasse, C. J. Dirksen, M. E. Brenchley, and M. T. Weller, *Chem. Phys. Lett.*, **234,** 177 (1995).
[23] H. J. Watzke and J. H. Fendler, *J. Phys. Chem.*, **91,** 854 (1987).
[24] B. A. Korgel and H. G. Monbouquette, *J. Phys. Chem.*, **100,** 346 (1996).

[25] K. M. Choi and K. J. Shea, *J. Phys. Chem.*, **98,** 3207 (1994).
[26] S. W. Haggata, X. Li, J. R. Fry, and D. J. Cole-Hamilton, *J. Mater. Chem.*, **6,** 1771 (1996).
[27] Y. Wang, A. Suna, W. Mahler, and R. Kasowski, *J. Chem. Phys.*, **87,** 7315 (1987).
[28] M. A. Olshavsky and H. R. Allcock, *Chem. Mater.*, **9,** 1367 (1997).
[29] P. C. Sercel, W. A. Saunders, H. A. Atwater, K. J. Vahala, and R. C. Flagan, *Appl. Phys. Lett.*, **61,** 696 (1992).
[30] O. V. Salata, P. J. Dobson, P. J. Hull, and J. L. Hutchison, *Adv. Mater.,* **6,** 772 (1994).
[31] O. V. Salata, P. J. Dobson, P. J. Hull, and J. L. Hutchison, *Thin Solid Films*, **251,** 1 (1994).
[32] N. L. Pickett, D. F. Foster, and D. J. Cole-Hamilton, *J. Mater. Chem.*, **6,** 507 (1996).
[33] J. E. Bowen-Katari, V. L. Colvin, and A. P. Alivisatos, *J. Phys. Chem.*, **98,** 4109 (1994).
[34] J. Hambrock, A. Birkner, and A. Fischer, *J. Mater. Chem.*, **11,** 3197 (2001).
[35] A. A. Guzelian, J. E. B. Katari, A. V. Kadavanich, U. Banin, K. Hamid, E. Juban, A. P. Alivisatos, R. H. Wolters, C. C. Arnold, and J. R. Heath, *J. Phys. Chem.*, **100,** 7212 (1996).
[36] A. A. Guzelian, U. Banin, A. V. Kadavinach, X. Peng, and A. P. Alivisatos, *Appl. Phys. Lett.*, **69,** 1432 (1996).
[37] R. E. Treece, S. G. Macala, L. Rao, D. Franke, H. Eckert, and R. B. Kaner, *Inorg. Chem.*, **32,** 2745 (1993).
[38] R. L. Wells, S. R. Aubuchon, S. S. Kher, M. S. Lube, and P. White, *Chem. Mater.*, **7,** 793 (1995).
[39] A. A. Guzelian, U. Banin, A. V. Kadavanich, X. Peng, and A. P. Alivisatos, *Appl. Phys. Lett.*, **69,** 1432 (1997).
[40] U. Banin, J. C. Lee, A. A. Guzelian, A. V. Kadavanich, and A. P. Alivisatos, *Superlattices and Microstructures*, **22,** 1294 (1997).
[41] M. A. Olshavsky, A. N. Goldstein, and A. P. Alivisatos, *J. Am. Chem. Soc.*, **112,** 9438 (1990).
[42] S. Schulz, L. Martinez, and J. L. Ross, *Adv. Mater. Opt. Electron.*, **6,** 185 (1996).
[43] M. A. Malik and P. O'Brien, *Adv. Mater. Opt. Electron.*, **3,** 171 (1994).
[44] D. M. Frigo, O. F. Z. Khan, and P. O'Brien, *J. Cryst. Growth,* **96,** 99 (1989).
[45] M. B. Hursthouse, M. A. Malik, M. Motevalli, and P. O'Brien, *Polyhedron,* **11,** 45 (1992).
[46] T. Trindade, P. O'Brien, X. Zhang, and M. Motevalli, *J. Mater. Chem.*, **7,** 1011 (1997).
[47] T. Trindade and P. O'Brien, *Adv. Mater.*, **8,** 161 (1996).
[48] V. K. LaMer and R. H. Dinegar, *J. Am. Chem. Soc.*, **72,** 4847 (1950).
[49] M. Chunggaze, J. McAleese, P. O'Brien, and D. Otway, *J. Chem. Soc. Chem. Comm.*, 833 (1998).
[50] T. Trindade, P. O'Brien, X. Zhang, and M. Motevalli, *J. Mater. Chem.,* **7,** 1011 (1997).
[51] N. Revaprasadu, M. A. Malik, and P. O'Brien, *Adv. Mater.*, **11,** 1441 (1999).
[52] M. A. Hines and P. Guyot-Sionnest, *J. Phys. Chem. B*, **102,** 3655 (1998).
[53] M. Chunggaze, M. A. Malik, and P. O'Brien, *J. Mater. Chem.*, **9,** 2433 (1999).
[54] B. Ludolph, M. A. Malik, P. O'Brien, and N. Revaprasadu, *J. Chem. Soc. Chem. Commun.*, 1849 (1998).
[55] M. A. Malik, N. Revaprasadu, and P. O'Brien, *Chem. Mater.*, **13,** 913, 2001.
[56] U. Banin, M. Bruchez, A. P. Alivisatos, T. Ha, S. Weiss, and D. S. Chemia, *J. Chem. Phys.*, **110,** 1195 (1999).
[57] M. A. Malik, P. O'Brien, and N. Revaprasadu, *J. Mater. Chem.*, **12,** 92 (2002).
[58] P. Sreekumari Nair, T. Radhakrishnan, N. Revaprasadu, G. A. Kolawole, and P. O'Brien, *Polyhedron*, **22,** 3129 (2003).

[59] P. S. Nair, T. Radhakrishnan, N. Revaprasadu, G. A. Kolawole, and P. O'Brien, *J. Mater. Chem.*, **12,** 1 (2002).

[60] S. L. Cumberland, K. M. Hanif, A. Javier, G. A. Khitrov, G. F. Strouse, S. M. Woessner, and C. S. Yun, *Chem. Mater.*, **14,** 1576 (2002).

[61] N. Revaprasadu, M. A. Malik, P. O'Brien, M. M. Zulu, and G. Wakefield, *J. Mater. Chem.*, **8,** 1885 (1998).

[62] B. Ludolph, M. A. Malik, P. O'Brien, and N. Revaprasadu, *J. Chem. Soc. Chem. Commun.*, 1849 (1998).

[63] D. Cupertino, D. J. Birdsall, A. M. Z. Slawin, and J. D. Woollins, *Inorg. Chim. Acta.*, **290,** 1 (1999).

[64] P. Bhattacharyya, J. Novosad, J. Phillips, M. L. Slawin, D. Williams, and J. Derek Woolins, *J. Chem. Soc., Dalton Trans.*, 1607 (1995).

[65] M. Afzaal, S. M. Aucott, D. Crouch, P. O'Brien, J. D. Woollins, and J. H. Park, *Chem. Vap. Deposition*, **8,** 187 (2002).

[66] M. Afzaal, D. Crouch, P. O'Brien, J. H. Park, *Mater. Res. Soc. Symp. Proc.*, 692 (2002).

[67] K. Osakada and T. Yamamoto, *J. Chem. Soc. Chem. Commun.*, 1117 (1987).

[68] J. G. Brennan, T. Siegrist, P. J. Carroll, S. M. Stuczynski, P. Reynders, L. E. Brus, and M. L. Steigerwald, *Chem. Mater.*, **2,** 403 (1990).

[69] D. J. Crouch, P. O'Brien, M. A. Malik, P. J. Skabara, and S. P. Wright, *J. Chem. Soc. Chem. Commun.,* 1454 (2003).

[70] P. Sreekumari Nair, N. Revaprasadu, T. Radhakrishnan, G. A. Kolawole, and P. O'Brien, *J. Chem. Soc. Chem. Comm.*, 564 (2002).

[71] Z. Peng and X. Peng, *J. Am. Chem. Soc.*, **124,** 3343 (2002).

[72] J. Yang, J. H. Zeng, S. H. Yu, L. Yang, G. Zhou, and Y. Qian, *Chem. Mater.*, **12,** 3259 (2000).

[73] S. H. Yu, S. H. Wu, J. Yang, Z. H. Han, Y. Xie, Y. Qian, and X. Liu, *Chem. Mater.*, **10,** 2309 (1998).

[74] S. D. Bunge, K. M. Krueger, T. J. Boyle, M. A. Rodriguez, T. J. Headley, and V. Colvin, *J. Mater. Chem.*, **13,** 1705 (2003).

[75] Y. Li, X. Li, C. Yang, and Y. Li, *J. Mater. Chem.*, **13,** 2641 (2003).

[76] X. G. Peng, L. Manna, W. D. Yang, J. Wickham, J. Scher, A. Kadavanich, and A. P. Alivisatos, *Nature*, **404,** 59 (2000).

[77] A. Sashchiuk, L. Amirav, M. Bashouti, M. Krueger, U. Sivan, and E. Lifshitz, *Nanoletters*, **4,** 159 (2004).

[78] R. L. Wells, C. G. Pitt, A. T. Mc Phail, A. P. Purdy, S. Shafieezad, and H. B. Hallock, *Chem. Mater.*, **1**, 4 (1989).

[79] M. Green, S. Norager, P. Moriarity, M. Motevalli, and P. O'Brien, *J. Mater. Chem.*, **10,** 1939 (2000).

[80] M. A. Malik, P. O'Brien, S. Norager, and J. Smith, *J. Mater. Chem.*, **13**, 2591 (2003).

[81] M. A. Malik, M. Afzaal, P.O'Brien, B. Hamilton, and U. Bangert, *J. Sci. Technol.*, (submitted).

[82] M. A. Malik and P. O'Brien (unpublished).

[83] M. Green and P. O'Brien, *J. Chem. Soc. Chem. Commun.*, 2459 (1998).

[84] M. Green and P. O'Brien, *Adv. Mater.*, **10,** 527 (1998).

[85] M. Green and P. O'Brien, *J. Mater. Chem.*, **9,** 243 (1999).

[86] O. I. Micic, J. R. Sprague, C. J. Curtis, K. M. Jones, J. L. Machol, A. J. Nozik, H. Giessen, B. Fluegel, G. Mohs, and N. J. Peyghambarian, *J. Phys. Chem.*, **99,** 7754 (1995).

[87] J. F. Janik, R. L. Wells, J. L. Coffer, J. V. St. John, W. T. Pennington, and G. L. Schimek, *Chem. Mater.*, **10,** 1613 (1998).

[88] A. Frank, F. Stowasser, H. Sussek, H. Pritzkow, C. R. Miskys, O. Ambacher, M. Giersig, and R. Fischer, *J. Am. Chem., Soc*, **120,** 3512 (1998).

[89] O. I. Micic, S. P. Ahrenkiel, D. Bertram, and A. J. Nozik, *App. Phys. Lett.*, **75,** 478 (1999).

[90] J. Wang, L. Grocholl, and E. G. Gillian, *Nanoletters*, **2,** 899 (2002).

[91] K. L. Stamm, J. C. Garno, G. Liu, and S. L. Brock, *J. Am. Chem. Soc.*, **125**, 4038 (2003).

[92] R. N. Bhargava, D. Gallagher, and T. Welker, *Phys. Rev. Lett.*, **72,** 416 (1994).

[93] K. Sooklal, B. S. Cullum, S. M. Angel, and C. J. Murphy, *J. Phys. Chem.*, **100,** 4551 (1996).

[94] D. Gallagher, W. E. Heady, J. M. Jacz, and R. N. Bhargava, *J. Cryst. Growth.*, **138,** 970 (1994).

[95] Y. L. Soo, Z. H. Ming, S. W. Huang, Y. H. Kao, R. N. Bhargava, and D. Gallagher, *Phys. Rev.*, **B 50**, 7602 (1994).

[96] A. A. Khosravi, M. Kundu, P. D. Vyas, S. K. K. Ulakarni, G. S. Shekhawat, R. P. Gupta, and A. K. Sharma, *Appl. Phys. Lett.*, **67,** 2506 (1995).

[97] Y. Wang, N. Herron, K. Moller, and T. Bein, *Solid State Commun.*, **77,** 33 (1991).

[98] L. Levy, N. Feltin, D. Ingert, and M. P. Pileni, *J. Phys. Chem. B*, **101,** 9153 (1997).

[99] G. Counio, T. Gacoin, and J. P. Boilot, *J. Phys. Chem.*, **102,** 5237 (1998).

[100] L. Levy, N. Feltin, D. Ingert, and M. P. Pileni, *Adv. Mater.*, **10,** 531 (1998).

[101] L. Levy, N. Feltin, D. Ingert, and M. P. Pileni, *Langmuir,* **15,** 3386 (1999).

[102] P. S. Nair, T. Radhakrishnan, N. Revaprasadu, G. A. Kolawole, and P. O'Brien, *J. Mater. Chem.*, **14,** 581 (2004).

[103] N. Revaprasadu, M. A. Malik, and P. O'Brien, *Mat. Res. Soc. Symp. Proc.*, 353 (1999).

[104] N. Revaprasadu, M. A. Malik, and P. O'Brien, *J. Mater. Chem.*, **11,** 2382 (2001).

[105] H. Weller, U. Koch, M. Gutierrez, and A. Henglein, *Ber. Bunsen-Ges. Phys. Chem.*, **91,** 88 (1987).

[106] A. Hasselbarth, A. Eychmuller, R. Eichburger, M. Giesi, A. Mews, and H. Weller, *J. Phys. Chem.*, **97,** 5333 (1993).

[107] A. Hasselbarth, A. Eychmuller, and H. Weller, *J. Luminescence*, **53,** 112 (1992).

[108] H. S. Zhou, I. Honma, H. Sahasahara, H. Komiyama, and J. W. Kraus, *Chem. Mater.*, **6,** 1534 (1994).

[109] M. A. Hines and P. Guyot-Sionnest, *J. Phys. Chem.*, **100,** 468 (1996).

[110] A. R. Kortan, R. Hull, R. L. Opila, M. G. Bawendi, M. L. Steigerwald, P. J. Carrol, and L. E. Brus, *J. Am. Chem. Soc.*, **112,** 1327 (1990).

[111] N. Revaprasadu, M. A. Malik, P. O'Brien, and G. Wakefield, *J. Chem. Soc. Chem. Comm.*, 1573 (1999).

[112] N. Revaprasadu, M. A. Malik, and P. O'Brien, *Chem. Mater.*, **14**, 2004 (2002).